Low-loss buried AlGaAs/AlOx waveguides using a quasi-planar process

Stéphane Calvez, Pierre-François Calmon, Alexandre Arnoult, Olivier Gauthier-Lafaye, Chantal Fontaine, Guilhem Almuneau

▶ **To cite this version:**

Stéphane Calvez, Pierre-François Calmon, Alexandre Arnoult, Olivier Gauthier-Lafaye, Chantal Fontaine, et al.. Low-loss buried AlGaAs/AlOx waveguides using a quasi-planar process. Optics Express, 2017, 25 (16), pp.19275 - 19275. 10.1364/OE.25.019275 . hal-01611629

HAL Id: hal-01611629
https://laas.hal.science/hal-01611629

Submitted on 6 Oct 2017

HAL is a multi-disciplinary open access archive for the deposit and dissemination of scientific research documents, whether they are published or not. The documents may come from teaching and research institutions in France or abroad, or from public or private research centers.

L'archive ouverte pluridisciplinaire **HAL**, est destinée au dépôt et à la diffusion de documents scientifiques de niveau recherche, publiés ou non, émanant des établissements d'enseignement et de recherche français ou étrangers, des laboratoires publics ou privés.

Low-loss buried AlGaAs/AlOx waveguides using a quasi-planar process

STEPHANE CALVEZ,[1] PIERRE-FRANCOIS CALMON, ALEXANDRE ARNOULT, OLIVIER GAUTHIER-LAFAYE, CHANTAL FONTAINE AND GUILHEM ALMUNEAU

[1] *LAAS, Univ de Toulouse, CNRS, 7 avenue du colonel Roche, F-31400 Toulouse, FRANCE*

**scalvez@laas.fr*

Abstract: In this letter, we demonstrate that buried oxide-confined waveguides can be formed using a lateral oxidation process carried out through a discrete set of small-diameter via holes instead of the conventional scheme where the oxidation starts from the edges of etched mesas. The via-hole oxidation is shown to lead to straight waveguides with smooth oxide/semiconductor interfaces and whose propagation losses are similar to the one obtained using the standard process but with the advantage of maintaining a quasi-planar wafer surface. It thereby paves the way towards a simplification of the fabrication of III-V-semiconductor-oxide photonic devices.

© 2017 Optical Society of America

OCIS codes: (230.7370) Waveguides, (130.0130) Integrated optics, (130.3130) Integrated optics materials

References and links

1. J. M. Dallesasse and N. Holonyak, "Oxidation of Al-bearing III-V materials: A review of key progress," J. Appl. Phys. **113**, 051101 (2013).
2. D. L. Huffaker, D. G. Deppe, K. Kumar, and T. J. Rogers, "Native-oxide defined ring contact for low threshold vertical-cavity lasers," Appl. Phys. Lett. **65**, 97 (1994).
3. J. M. Dallesasse and D. G. Deppe, "III-V Oxidation: Discoveries and Applications in Vertical-Cavity Surface-Emitting Lasers," Proc. IEEE **101**, 2234–2242 (2013).
4. S. A. Maranowski, A. R. Sugg, E. I. Chen, and N. Holonyak, "Native oxide top- and bottom-confined narrow stripe p-n AlyGa1−yAs-GaAs-InxGa1−xAs quantum well heterostructure laser," Appl. Phys. Lett. **63**, 1660 (1993).
5. K. De Mesel, R. Baets, C. Sys, S. Verstuyft, I. Moerman, and P. Van Daele, "First demonstration of 980 nm oxide confined laser with integrated spot size converter," Electron. Lett. **36**, 1028 (2000).
6. S. J. Caracci, M. R. Krames, N. Holonyak, C. M. Herzinger, A. C. Crook, T. A. DeTemple, and P. -A. Besse, "Native-oxide-defined low-loss AlGaAs-GaAs planar waveguide bends," Appl. Phys. Lett. **63**, 2265–2267 (1993).
7. M. R. Krames, E. I. Chen, N. Holonyak, A. C. Crook, T. A. DeTemple, and P. -A. Besse, "Deep-oxide planar buried-channel AlGaAs–GaAs quantum well heterostructure waveguides with low bend loss," Appl. Phys. Lett. **66**, 1912–1914 (1995).
8. C. L. Chua, R. L. Thornton, and D. W. Treat, "Planar laterally oxidized vertical-cavity lasers for low-threshold high-density top-surface-emitting arrays," IEEE Photonics Technol. Lett. **9**, 1060–1062 (1997).
9. S. N. Tandon, J. T. Gopinath, H. M. Shen, G. S. Petrich, L. A. Kolodziejski, F. X. Kärtner, and E. P. Ippen, "Large-area broadband saturable Bragg reflectors by use of oxidized AlAs," Opt. Lett. **29**, 2551–2553 (2004).
10. S. P. Nabanja, L. A. Kolodziejski, and G. S. Petrich, "Lateral Oxidation of AlAs for Circular and Inverted Mesa Saturable Bragg Reflectors," IEEE J. Quantum Electron. **49**, 731–738 (2013).
11. F. Chouchane, H. Makhloufi, S. Calvez, C. Fontaine, and G. Almuneau, "Photoluminescence from InGaAs/GaAs quantum well regrown on a buried patterned oxidized AlAs layer," Appl. Phys. Lett. **104**, 061912 (2014).
12. S. Calvez, G. Lafleur, A. Larrue, P.-F. Calmon, A. Arnoult, G. Almuneau, and O. Gauthier-Lafaye, "Vertically Coupled Microdisk Resonators Using AlGaAs/AlOx Technology," IEEE Photonics Technol. Lett. **27**, 982–985 (2015).
13. A. B. Fallahkhair, K. S. Li, and T. E. Murphy, "Vector Finite Difference Modesolver for Anisotropic Dielectric Waveguides," J. Light. Technol. **26**, 1423–1431 (2008).
14. M. J. Cich, R. Zhao, E. H. Anderson, and E. R. Weber, "Influence of gas transport on the oxidation rate of aluminum arsenide," J. Appl. Phys. **91**, 121 (2002).

15. G. Almuneau, R. Bossuyt, P. Collière, L. Bouscayrol, M. Condé, I. Suarez, V. Bardinal, and C. Fontaine, "Real-time in situ monitoring of wet thermal oxidation for precise confinement in VCSELs," Semicond. Sci. Technol. **23**, 105021 (2008).
16. F. Chouchane, G. Almuneau, N. Cherkashin, A. Arnoult, G. Lacoste, and C. Fontaine, "Local stress-induced effects on AlGaAs/AlOx oxidation front shape," Appl. Phys. Lett. **105**, 041909 (2014).
17. D. Liang and D. C. Hall, "Reduction of etched AlGaAs sidewall roughness by oxygen-enhanced wet thermal oxidation," Appl. Phys. Lett. **91**, 061110 (2007).
18. B. W. Hakki and T. L. Paoli, "cw degradation at 300°K of GaAs double-heterostructure junction lasers. II. Electronic gain," J. Appl. Phys. **44**, 4113–4119 (1973).
19. C. Ozanam, M. Savanier, L. Lanco, X. Lafosse, G. Almuneau, A. Andronico, I. Favero, S. Ducci, and G. Leo, "Toward an AlGaAs/AlOx near-infrared integrated optical parametric oscillator," J. Opt. Soc. Am. B **31**, 542–550 (2014).
20. P.-C. Ku, J. Hernandez, and C. Chang-Hasnain, "Buried selectively-oxidized AlGaAs structures grown on nonplanar substrates," Opt. Express **10**, 1003 (2002).
21. Guang-Hua Duan, C. Jany, A. Le Liepvre, A. Accard, M. Lamponi, D. Make, P. Kaspar, G. Levaufre, N. Girard, F. Lelarge, J.-M. Fedeli, A. Descos, B. Ben Bakir, S. Messaoudene, D. Bordel, S. Menezo, G. de Valicourt, S. Keyvaninia, G. Roelkens, D. Van Thourhout, D. J. Thomson, F. Y. Gardes, and G. T. Reed, "Hybrid III--V on Silicon Lasers for Photonic Integrated Circuits on Silicon," IEEE J. Sel. Top. Quantum Electron. **20**, 158–170 (2014).

1. Introduction

The wet oxidation of aluminum-containing III-V semiconductors is an established and commercially exploited process which defines the electrical injection path and optical field distribution within semiconductor device structures [1] such as Vertical-Cavity Surface-Emitting Lasers (VCSELs) [2] [3] or optical waveguides [4] [5]. It relies on the local transformation a high-refractive-index ($n_{Al\text{-}III\text{-}V}$~2.9) semiconductor material into low-refractive-index (n_{AlOx}~1.6) insulating aluminum oxide (AlOx) by water vapor. Practically, this compositionally-selective oxidation proceeds from and progresses away from the exposed edges of etched mesas, transforming, at depth in the structure, (thin) buried Al-bearing semiconductor layers into AlOx. If the lateral extent of oxide is smaller than the mesa size, this process leads to the creation of buried oxide/semiconductor apertures which are then used to establish the desired device lateral electronic and optical confinements. The prime limitations of this technique are essentially related to the loss of the wafer surface planarity caused by the large and continuous corrugation of the sample surface introduced by the mesa structures. This can be avoided if the oxidation process is carried out from the wafer surface as in [6][7], but, in this case, only weakly-confined optical waveguides in the topmost section of (multi-plane) structures can be made.

Alternatively, to address this issue and ease the fabrication of VCSELs and VCSEL arrays, a quasi-planar variant of this process has been introduced in [8] where the oxidation is performed through a discrete set of small-diameter via-holes. Although unimportant for this application, the lateral oxide/semiconductor interfaces were rough as a result of the coarse hole distribution and short oxidation distance. Since then, the latter process has also been applied to create contiguous oxide regions with sparse surface disruption to make highly-reflective mirrors over large areas [9] [10] or to facilitate epitaxial regrowth [11]. Furthermore, the availability of a process able to create buried oxide structures whilst maintaining a quasi-planar surface is considered to be particularly attractive when making multi-plane photonic devices such as mode-converted laser diodes [5] or vertically-coupled resonators [12], especially when the device layout requires lithographically-defined patterns of high resolution.

In this context, we demonstrate in this letter that this via-hole oxidation process can be used to create oxide apertures with smooth lateral oxide/semiconductor interfaces and can thereby enable the fabrication of low-loss buried oxide-confined straight waveguides with the desired quasi-planar wafer surface.

2. Device design

The device vertical semiconductor structure was originally designed and grown (by molecular beam epitaxy (Riber 412) on GaAs (001)) to subsequently fabricate micro-disk resonators which are vertically-coupled to their buried oxide-confined access waveguide [12]. After a global etch of the resonator core layer and of part of its lower cladding layer, the multi-layer stack used here to create the oxide-confined waveguides consists, from bottom to top, of a 1.6µm-thick $Al_{0.7}Ga_{0.3}As$ bottom cladding layer, a 480-nm GaAs core, a 150-nm-thick $Al_{0.3}Ga_{0.7}As$ cladding, a 68 nm-thick $Al_{0.98}Ga_{0.02}As$ layer, a 330-nm-thick $Al_{0.3}Ga_{0.7}As$ layer, a second 68 nm-thick $Al_{0.98}Ga_{0.02}As$ layer and a final 50nm-thick $Al_{0.3}Ga_{0.7}As$ layer. Both $Al_{0.98}Ga_{0.02}As$ layers were oxidized simultaneously to form apertures.

The analysis of the waveguiding properties of the above-described structure using finite difference modelling [13] shows that devices with oxide apertures smaller than ~4.5 µm exhibit TE-polarized single lateral mode propagation.

It is worth pointing out here that the topmost oxide aperture plays negligible role in establishing the waveguide mode profile and effective index given its distance to the waveguide core but can be effectively used to monitor the oxide/semiconductor boundary profile given its proximity to the wafer surface.

3. Device Fabrication

The above described layer structure was post-processed in a single run to create oxide-confined waveguides using the conventional and the quasi-planar oxidation techniques, resulting in the devices represented in Fig. 1. In the quasi-planar case, the holes were distributed along two lines with a center-to-center separation of 38 µm and with either a regular hole-to-hole pitch (which was varied from device to device from 2.5 to 4.5 µm – see Fig.2 centre) or a randomly-selected hole-to-hole distance (in the 2.5 to 4.5 µm range - see Fig.2 right). The diameter of the holes was chosen to be 2 µm to be compatible with standard optical lithography and avoid reducing the oxidation rate by restricting the water/gas access to the $Al_{0.98}Ga_{0.02}As$/AlOx layers [14].

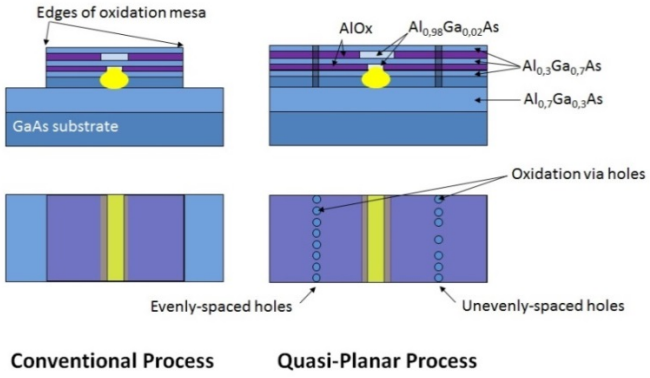

Fig. 1. Schematic cross-sections (up) and top-views (bottom) of the fabricated buried waveguide.

Following the simplistic yet common view that the oxidation boundary can be inferred from the mesa shape by homothetic transformation, the regularly-spaced hole patterns should lead, for sufficiently long oxidation, to overlapping circles creating a high-(grating)-order lateral distributed feedback (DFB) structure whose corrugation full width, Δw, is given by:

$$\Delta w = 2 \cdot D \cdot \left(1 - \sin\left(\cos^{-1}\left(\frac{D_{sep}}{2 \cdot D}\right)\right)\right) \quad (1)$$

where D_{sep} is the hole-to-hole separation, i.e. the grating pitch or the rugosity correlation length, and $D=D_{ox}+D_h/2$ with D_{ox} the oxidation distance, D_h the hole diameter.

The aperiodic structures were implemented to create DFB-free waveguides whose average peak-to-peak rugosity is given by Eq. (2) with D_{sep}=3.5µm and for which the correlation length was found to be 3.5 µm by calculating the Fourier-transform of the hole distribution.

The line patterns and desired discrete sets of holes were defined by direct laser writing (Heidelberg DWL 200) in SPR700 photoresist. These patterns were then transferred in the AlGaAs stack by ICP-RIE plasma etching using a $Cl_2/N_2/Ar$ gas mixture to open access to both $Al_{0.98}Ga_{0.02}As$ layers. The lateral wet oxidation was carried out using a 95°C mixed $H_2/N_2/H_2O$ gas steam generated by an evaporator-mixer system, the sample being held in a reduced pressure environment (~0.5 atm.) at a substrate temperature of 400°C. Using the in-situ monitoring system [15], the oxidation was stopped when the aperture of the conventionally-made waveguides reached ~4.0 µm corresponding to an oxidation distance of ~16 µm. We wish to emphasize that, using this equipment and upon calibration, a reproducibility of 0.2 µm is routinely achieved for this aperture size. After thinning the wafer down to ~150 µm, 2050-µm-long waveguides were cleaved and mounted on Si sub-mounts.

4. Device characterisation and discussion

Figure 2 shows optical microscope images of the fabricated oxide-confined waveguides. Given the absorption of the AlGaAs alloys in the visible region, only the topmost oxide aperture can be observed and can be measured to be ~7.2µm wide. SEM images (not shown here but in [12]) show that the lower aperture is smaller (~4.5 µm) due to a slight (<0.35%) difference in composition between the nominally identical $Al_{0.98}Ga_{0.02}As$ layers and because of strain-induced effects [16].

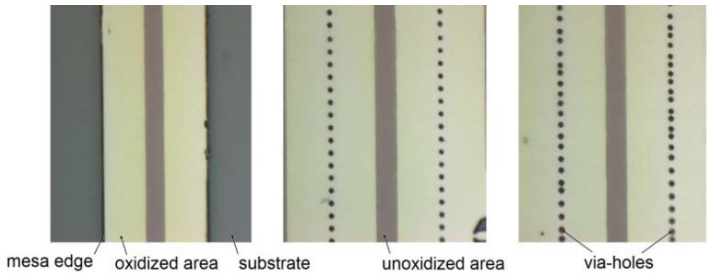

Fig. 2. Optical microscope images of oxide-confined waveguides made by (left) the conventional process, by the quasi-planar process with (middle) 4.3-µm-pitch holes and (right) irregularly-spaced holes. The width of the mesa is 36 µm and the distance between the lines of holes is 38 µm.

Figure 2 also suggests that the boundary between the oxidized and unoxidized areas is straight independently of the fabrication method (conventional or quasi-planar). Furthermore, exploiting the fact that the oxidation induces a volume contraction, surface profilometry of the produced waveguides using atomic force microscopy was used to extract with greater accuracy the shape of the oxidation boundaries. A double-step profile, with an inner width of ~4.5 µm and outer width of ~7.2 µm corresponding respectively to the bottom and top apertures, can be distinguished from the presented map and average vertical profile of Fig. 3. Extracting the oxide-semiconductor boundaries using image processing edge detection techniques on a higher resolution image confirms that the quasi-planar process leads to linear oxidation fronts with sub-7-nm rugosity. This experimental observation and, in particular, the difference between the measured and calculated (using Eq. (2)) corrugations can be understood as a direct consequence of the smoothing effects introduced by the diffusive nature of the oxidation process [17].

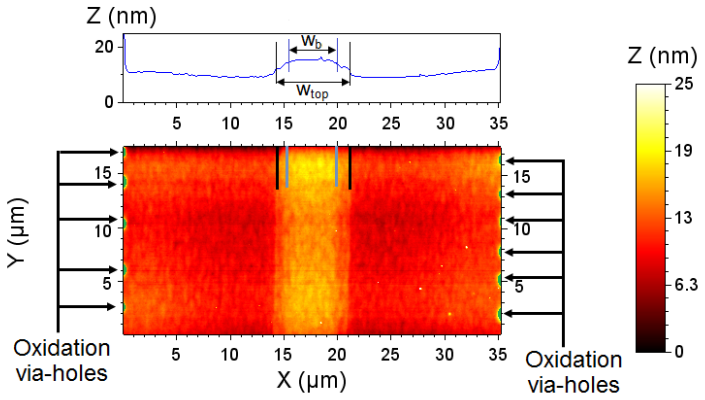

Fig. 3. Atomic Force Microscope image of a section of the $Al_{0.98}Ga_{0.02}As$/AlOx boundary of a waveguide with unevenly-spaced oxidation via-holes. The averaged vertical profile is shown in the top insert. The hole distribution is highlighted (X~0μm and ~35μm). The widths of the two oxide apertures are also highlighted (in blue and black).

Using the setup shown Fig. 4, the fibre-to-fibre (A to B) optical transmission characteristics were then measured in with a 1 pm spectral resolution using a tunable laser with central wavelength of 1.6 μm and a 100 kHz linewidth. The close similarity of the recorded fringe patterns (see Fig. 4) suggests that waveguide performance is not significantly affected by the fabrication method and that the process and sample preparation were performed with good uniformity. The noticeable long-range envelop fluctuations are induced by the fiber-part of the setup as the fringe maxima and minima share the same (scaled) power variation pattern.

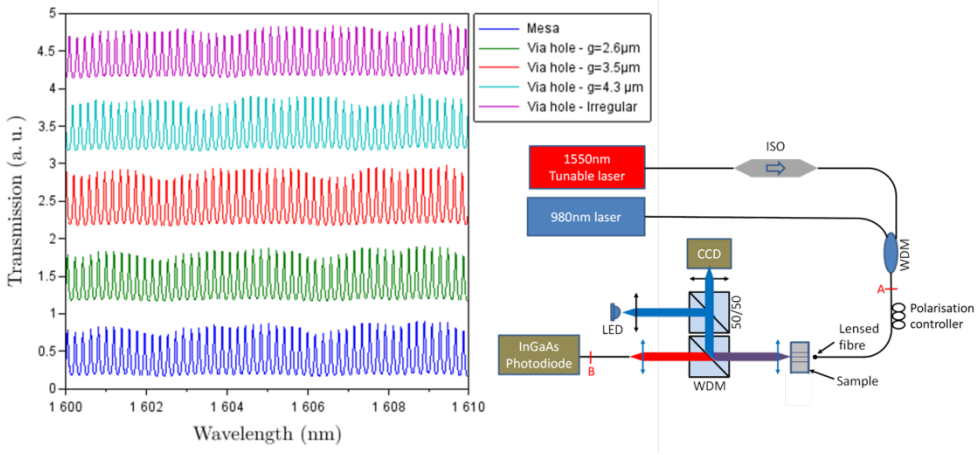

Fig. 4. Fibre-to-fibre transmission characteristics including the fabricated waveguides measured using the represented setup.

It is worth pointing out however that the recorded spectra of the waveguides made using the regular hole distribution do not present any DFB signature. This is consistent with the above-described AFM observation. Indeed, given that the AlOx/AlAs boundary was found to exhibit a corrugation smaller than 7 nm, and having calculated that the effective index spectral and width dependence of the fundamental mode can be approximated described (with an accuracy better than 10^{-4} in index value) using the following parabolic relationship:

$$n_{eff}(\lambda, w) = n_0 + a_1\lambda + a_2\lambda^2 + b_1 w + b_2 w^2 \quad (2)$$

where λ is the wavelength (ranging from 1.5 to 1.63μm), and w is the aperture width (ranging

from 2.5 to 5µm), n_0=3.8428, a_1=-0.582 µm^{-1}, a_2=0.133 µm^{-2}, b_1=2.951 10^{-3} µm^{-1}, and b_2=-2.43 10^{-4} µm^{-2}, the maximum resulting waveguide effective index modulation can be estimated to be Δn_{eff}=1.4 10^{-5}. The stopband bandwidth supported by the DFB pattern can then be evaluated using the following expression: $\Delta\lambda_{DBR} = 4\lambda/M\pi \,\mathrm{SIN}^{-1}\left(\Delta n_{eff}/2n_{eff}\right)$ where M is the grating order. For a device with a 4.5µm pitch (M=9), it could therefore reach 1.38 pm. The latter value, at best, approaches the spectral resolution in use for the transmission measurements and justifies that this effect could not be detected here.

The free spectral range (FSR) measured from the Fabry-Perot fringes is of 190 pm and is in good agreement with the 187 pm anticipated from the calculated effective refractive index (Eq. 2) and chip length. It is found to be constant over the considered spectral range which dismisses multimode operation.

The propagation losses of the fabricated waveguides were extracted from measurements on ~150 fringes using standard Fabry-Perot analysis [18] using a calculated cleaved-facet reflectivity value of 39.0%. Being a contrast analysis, this data treatment also eliminates the long-range (>0.5*FSR) weak power variations. The results are shown to be ~0.45 cm^{-1} (Fig. 5), on a par with other record low-loss AlOx/GaAs waveguides [19]. The losses only rise slightly for the quasi-planar waveguides with the most widely-spaced via-hole separation (>4 µm) for which the corrugation amplitude is expected to be the greatest (see Eq. (1)).

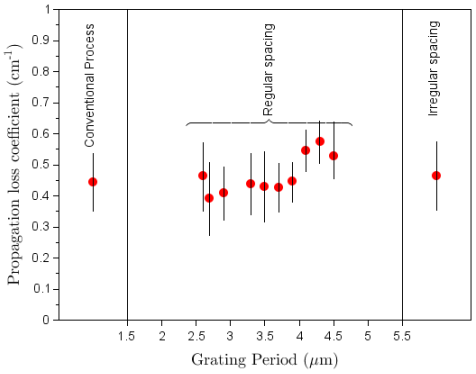

Fig. 5. Loss characteristics of the straight waveguides produced by the standard and the quasi-planar oxidation processes. The error bars represent the standard deviation error over the measured ~150 fringes.

5. Conclusions

We have demonstrated that buried oxide-confined waveguides can be formed using a lateral oxidation process carried out through a discrete set of small-diameter via holes instead of the conventional scheme where the oxidation starts from the edges of an etched mesa ridge. This via-hole oxidation enables the fabrication of straight waveguides whose propagation losses are similar to the ones obtained using the standard ridge process but with the advantage of maintaining a quasi-planar wafer surface. Furthermore, using a commensurable hole pitch and oxidation extent , the presented process could lead to periodically corrugated boundaries [11] and, thereby, enable the fabrication of (high-order) DFB structures in a simpler way than in [20]. In both cases, this process is expected to ease the fabrication of more advanced III-V-semiconductor-oxide photonic devices, especially when they rely on multi-plane structures [12] or when they require epi-side-down mounting or hybrid integration [21].

Funding

The French National Space Agency CNES (R&T contract “frequency combs on a chip”); The French RENATECH network of micro-fabrication facilities.